Surface and Coatings Technology **73** (1995) 152-159

Low Friction, High Endurance Ion-Beam Deposited Pb-Mo-S Coatings

K.J. Wahl*, L.E. Seitzman, R.N. Bolster, and I.L. Singer
Code 6170, U.S. Naval Research Laboratory, Washington, DC 20375-5342

* NRC/NRL Postdoctoral Research Associate
Received 3 June 1994; accepted in final form 11 October 1994

Abstract

Thin solid lubricating coatings of Pb-Mo-S were deposited on steel substrates via ion-beam deposition. Coating endurance and friction coefficients under dry air sliding conditions were monitored with ball-on-disk tests; additional tribological testing was performed using a ball-on-flat reciprocating test rig to investigate intermediate sliding distances (100-32000 cycles). Rutherford backscattering spectrometry (RBS), X-ray diffraction (XRD), scanning Auger microscopy, and micro-Raman spectroscopy were used to examine structure, composition, and chemistry of the coatings. Worn surfaces were characterized with optical microscopy and micro-Raman spectroscopy. Average endurance (at 1.4 GPa stress) of ion-beam deposited (IBD) Pb-Mo-S coatings 160-830 nm thick containing from 4-26 at.% Pb was 160000 revolutions, more than 2 times that of IBAD (ion-beam-assisted deposition) MoS_2 coatings. Additionally, the IBD Pb-Mo-S coatings had friction coefficients between 0.005 and 0.02, similar to the IBAD MoS_2 coatings. Friction coefficients were monitored as a function of contact stress and found to obey the Hertzian contact model; measured interfacial shear strengths (S_0~12 MPa) were similar to those observed for MoS_2 coatings. Although XRD and micro-Raman spectroscopy indicated that the IBD Pb-Mo-S coatings were initially amorphous, micro-Raman spectroscopy showed that crystalline MoS_2 was produced both in the wear tracks on coatings and in the transfer films on balls after as few as 100 sliding cycles. The wear resistance and low friction properties of IBD Pb-Mo-S coatings are attributed to the combination of dense, adherent coatings and formation of easily-sheared, MoS_2-containing sliding surfaces.

Keywords: Ion beam deposition; Pb-Mo-S coatings

1. Introduction

For many years, researchers have demonstrated that by mixing and/or alloying MoS_2 with other materials, low friction can be maintained while endurance is improved. Simple mechanical alloying of MoS_2 with graphite [1] is an early example; other additions include compounds such as Sb_2S_4 [2,3], which improved high temperature performance. Early sputter deposition techniques employed small amounts of metal additives (e.g. Ni [4], Au [5]) and even PTFE [6]. More recently, sophisticated deposition techniques such as multilayering of metals in MoS_2 coatings have been developed [7]. Additionally, laser ablation and pulsed laser deposition techniques have been employed to alloy MoS_2 [8,9] and oxides [10,11] with metals. All of the alloying techniques mentioned above can result in improved friction and endurance performance over similarly prepared unalloyed coatings.

Previous investigations [12,13] have shown that IBAD MoS_2 coatings provide both low friction and superior endurance for tribological applications. The present study demonstrates the potential to improve IBAD MoS_2 coatings by alloying with Pb. Friction and endurance of the alloyed coatings and the relationship to Pb content and processing method are examined. Analytical studies which reveal the structure and chemistry of the coatings and worn surfaces are presented.

2. Experimental Procedure

Pb-Mo-S coatings were deposited by dual ion beam deposition in a vacuum chamber equipped with three Kaufman argon ion sources. In this ion-beam-assisted

Report Documentation Page

Form Approved
OMB No. 0704-0188

1. REPORT DATE	2. REPORT TYPE	3. DATES COVERED
1995		**00-00-1995 to 00-00-1995**

4. TITLE AND SUBTITLE	5a. CONTRACT NUMBER
Low Friction, High Endurance Ion-Beam Deposited Pb-Mo-S Coatings	5b. GRANT NUMBER
	5c. PROGRAM ELEMENT NUMBER
6. AUTHOR(S)	5d. PROJECT NUMBER
	5e. TASK NUMBER
	5f. WORK UNIT NUMBER
7. PERFORMING ORGANIZATION NAME(S) AND ADDRESS(ES) **Naval Research Laboratory,Code 6170,4555 Overlook Avenue, SW,Washington,DC,20375**	8. PERFORMING ORGANIZATION REPORT NUMBER
9. SPONSORING/MONITORING AGENCY NAME(S) AND ADDRESS(ES)	10. SPONSOR/MONITOR'S ACRONYM(S)
	11. SPONSOR/MONITOR'S REPORT NUMBER(S)

12. DISTRIBUTION/AVAILABILITY STATEMENT
Approved for public release; distribution unlimited

13. SUPPLEMENTARY NOTES

14. ABSTRACT

15. SUBJECT TERMS

16. SECURITY CLASSIFICATION OF:			17. LIMITATION OF ABSTRACT	18. NUMBER OF PAGES	19a. NAME OF RESPONSIBLE PERSON
a. REPORT **unclassified**	b. ABSTRACT **unclassified**	c. THIS PAGE **unclassified**		**8**	

deposition system, two of the ion beams are focused on separate sputtering targets, while the third ion gun provides a broad beam for sputter cleaning the substrates prior to deposition as well as functions as an assist ion beam during deposition [12,14]. While deposition of dual-element coatings can be accomplished by simply having two different targets of the desired elements (e.g. Mo and S for MoS_2 coatings), deposition of three components requires more specialized targets. For this experiment, two different target configurations were used: (1) Pb and Mo-S (S powder melted into holes in a Mo target) and (2) MoS_2 and Pb. In the second configuration (MoS_2 and Pb), a larger sputtering power was needed on the MoS_2 target to obtain a reasonable deposition rate; this resulted in beam broadening at the target. Deposition of coatings is accomplished under vacuum conditions of 0.05 Pa; as a result, small amounts of oxygen and carbon are incorporated into the coatings (typically ~2 at.%). To reduce the number of operating parameter variables during deposition of the Pb-Mo-S coatings, 1) the assist ion gun was not used except to sputter clean the substrates, and 2) depositions were performed at room temperature, with modest increases (maximum 67°C) resulting from ion-beam heating. For clarity, the Pb-Mo-S coatings prepared without the assist ion gun will be referred to as IBD (ion-beam deposited) Pb-Mo-S.

The IBD Pb-Mo-S coatings were deposited on various hardened steel substrates (M50, 52100, 440C, and AMS 5749) to thicknesses from 160 to 830 nm. The coatings, containing between 4 and 50 at.% Pb, were compared to unalloyed IBAD MoS_2 as well as to a Pb coating. Some of the coatings also had a thin (30-40 nm) TiN interlayer [15]. Glass microscope slides (for thickness determination via interference microscopy over coating edge) and strips of Ni foil (for Rutherford backskattering spectrometry (RBS)) were placed near the steel substrates during deposition. Density was determined using measured coating thickness and RBS and was based on the theoretical densities of MoS_2, Pb and excess S or Mo [14]. Coating composition was determined by RBS depth profiling. Additional compositional analysis of selected coatings was performed using Auger spectroscopy and depth profiling. Coating structure was analyzed by X-ray diffraction (XRD) in standard $\theta/2\theta$ configuration, with a rotating Cu anode operated at 50 kV and 200 mA.

Coating endurance and friction behavior under unidirectional sliding contact were measured using a ball-on-disk tribometer. 52100 steel balls (3.18 mm in diameter) were cleaned in toluene, acetone and propanol prior to testing. The load was fixed at L = 9.8 N, giving a mean Hertzian stress of P_H = 1.4 GPa, and the sliding speed was 0.3 to 1.0 m/s. Coating endurance was defined as the number of revolutions before the friction coefficient reached 0.2. Typically 2-4 endurance tests were performed on each coating; these results were then averaged to obtain mean endurance values. Ball-on-disk experiments were also performed to acquire friction coefficient vs. load data. The Hertzian contact model [see e.g. 16] was used to determine the interfacial shear strength of the solid lubricating films from friction measurements according to $\mu = (S_o/P_H) + \alpha$ [17,18]. In this model, the friction coefficient is represented as a function of interfacial shear strength S_o, contact stress P_H, and pressure dependence of shear strength term α. The constants S_o and α represent material properties of the interface controlling friction; for ball-on-flat geometry under elastic contact conditions, $P_H \propto L^{-1/3}$.

Additional sliding tests on selected coatings were performed using a reciprocating ball-on-flat tribometer with 6.35 mm diameter steel balls, an initial load of 9.8 N (P_H = 0.92 GPa), and sliding speed of 4 mm/s. Some of the reciprocating tests were performed on coatings deposited on glass substrates as well, which results in somewhat lower stress (P_H = 0.57 GPa). Reciprocating sliding test lengths ranged from 100 cycles to 32000 cycles. Both tribometers were enclosed in glove boxes providing dry air (<2% RH) environments, obtained by flowing compressed air through desiccant columns and cold traps chilled in a dry ice + propanol mixture (-77°C, partial pressure water vapor = 0.08 Pa).

After reciprocating sliding tests, wear tracks on coatings and transfer films on balls were examined optically by interference (Nomarski) microscopy. Micro-Raman spectroscopy was performed on tracks and balls using a Renishaw imaging microscope equipped with a low power (<25 mW) Ar^+ laser (514 nm); spectrometer resolution was 1 cm^{-1}, and imaging optics provided spatial resolution of ~2 μm. Laser power levels were kept very low to ensure that observed crystalline material was not an artifact of laser beam heating of the coatings or debris material. Balls and tracks were examined in a Physical Electronics PHI 660 scanning Auger spectrometer. Auger spectra were acquired using an electron beam energy of 5 keV and sputter depth profiling with a 3 keV Ar^+ ion beam. Sensitivity factors provided by PHI were used to obtain normalized Auger intensities.

The various analytical techniques in this paper sample substantially different volumes of matter. The x-ray radiation used in XRD passes completely through the material, resulting in sampling of the entire coating and substrate. Auger electrons, on the other hand, have mean free paths of 1–2 nm for the elements of interest [19] and are therefore very surface sensitive.

While the depth sensitivities of XRD and Auger spectroscopy are well known, the sampling depth of Raman spectroscopy is dependent on the optical transparency of the material under investigation. The penetration depth, t_c, can be estimated using Beer's law and optical absorption coefficients (α') and is given by

$$I/Io = e^{-\alpha' t} \quad (1)$$

where $\alpha' t_c = 1$ [20]. Under the present experimental conditions, Raman signal is obtained in the backscattering mode. Therefore, the observed Raman signal sampling depth is $t_c/2$. While we do not know the optical properties of the IBD Pb-Mo-S coatings at this time, we can estimate the sampling depth by considering crystalline MoS_2. We consider the case of 514 nm photons incident on basally oriented MoS_2 ($\alpha' \sim 1.4 \times 10^5$ cm^{-1})[21]. This results in an estimate of maximum penetration depth for crystalline MoS_2 of $t_c \sim 70$ nm, which corresponds to ~35 nm Raman sampling depth. An upper bound of 55 nm was inferred experimentally when no Si peak could be detected from a 55 nm crystalline IBAD MoS_2 coating on single crystal Si.

3. Results

3.1. Friction and wear behavior

The endurances of IBD Pb-Mo-S coatings, for the various deposition conditions, are presented in Table 1. Mean endurances of coatings containing from 4 to 26 at.% Pb ranged from 9000 to 466000 revolutions. No trends between coating Pb content and endurance were noted for Pb concentrations below 26 at.%. The 50 at.% Pb-Mo-S coating and a 100% Pb coating failed almost immediately (<1000 revolutions). For comparison, the friction and endurance of IBD Pb-Mo-S and IBAD MoS_2 coatings are summarized in Table 2. The IBD Pb-Mo-S coatings had endurances much better than the average IBAD MoS_2 coatings. Moreover, the IBD Pb-Mo-S coatings had better average performances than the IBAD MoS_2 coatings developed by optimizing processing parameters [13].

The pin-on-disk friction behavior of the IBD Pb-Mo-S coatings under dry sliding conditions is similar to that of IBAD MoS_2 coatings [12]. In both cases, the friction coefficient decreases from the initial value to a steady minimum. The minimum friction measured for IBD Pb-Mo-S coatings containing from 4 to 26 at.% Pb ranged between 0.005 and 0.021. These values are similar to the minimum friction coefficients measured for IBAD MoS_2 coatings, as shown in Table 2 [12,13]. The 50 at.% Pb coating and the 100% Pb coating had much higher friction coefficients, 0.13 and 0.4 respectively.

The dependence of friction coefficient on load was examined for several IBD Pb-Mo-S coatings; the results of regression analysis and least-squares fits to the Hertzian contact model are shown in Table 3. The behavior was found to satisfy $\mu = L^{\beta}$; the coefficients $\beta = -0.33$ to -0.38 agree well with $\beta = -1/3$ expected for ball-on-flat geometry. Values for S_o (8 to 15 MPa) and α (0.001 to 0.010) of the IBD Pb-Mo-S coatings tested were similar to those observed for both IBAD MoS_2 as well as sputtered MoS_2 coatings; in fact, S_o values of 8 and 10 MPa for IBD Pb-Mo-S were some of the lowest measured among the coatings tested.

Table 1.
Pb-Mo-S coatings on steel.

Target onfiguration	Pb (%)	Substrate	Thickness (nm)	Endurance (krev)	m_{min}
Pb	100	AMS	405	0.098[c]	0.4
Pb, Mo+S	50[a]	440C	585	0.085, 1.1	0.13
	26	AMS	435	118 ± 50	0.015
	25[a]	440C	730	66 ± 10	0.020
	24	AMS	510	246, 248	0.013
	23	440C	745	45 ± 18	0.014
	22	M50	750	58 ± 21	0.020
	21	440C[b]	525	200 ± 14	0.015
	21	52100	785	456, 477	0.018
	19	52100	830	160, 136	0.021
	19	52100	785	87 ± 37	0.010
	19	M50[b]	500	182 ± 89	0.010
	17	52100	445	254 ± 66	0.005
	7	AMS[b]	435	87 ± 35	0.014
	21	440C	350	9.2 ± 4.4	0.013
	13	440C	335	260 ± 75	0.010
MoS_2 & Pb	11	440C	325	118 ± 18	0.009
	6	M50	300	188[c]	0.007
	4	M50	305	179[c]	0.011

[a]Pb content obtained via experimental calibration of deposition rates.
All other values are determined via RBS.
[b]30-40 nm TiN interlayer
[c]Result of 1 endurance experiment; all other results of 2-4 experiments.

Table 2.
Endurance of IBD Pb-Mo-S and IBAD MoS_2 coatings.

Coating Type	Endurance (kcycles)	m_{min}	Coating Number
IBD Pb-Mo-S (4-26 at.% Pb)	160±106	0.005–0.021	17
IBAD MoS_2 (all)	70±65	0.004–0.10	129
IBAD MoS_2 (optimized)	105±85	0.010–0.023	29

[a]Pb content 4-26 at.%

Table 3.
S_0, α and β values calculated using Hertzian contact model

Coating Type	S_0 (MPa)	α	$-\beta$
IBD Pb-Mo-S[a]	8 – 15	0.001–0.016	0.33– 0.38
IBAD MoS_2	12 – 23	0.001–0.012	0.33– 0.38
Sputtered MoS_2+Ni[b] [4]	9 – 35	0–0.015	0.32– 0.38

[a]4 – 18 at.% Pb content
[b]values for steel substrate/ball couples only [17]

Reciprocating sliding tests were performed on selected IBD Pb-Mo-S coatings to intermediate sliding distances (100 to 32000 cycles); a typical example is shown in Figure 1. Friction coefficients of IBD Pb-Mo-S coatings

were higher than IBAD MoS_2 during run-in (dropping steadily during the first 100 or so cycles); however, they were similar to the IBAD MoS_2 at steady state. For the relatively low speed reciprocating sliding, steady state friction coefficients were typically 0.05.

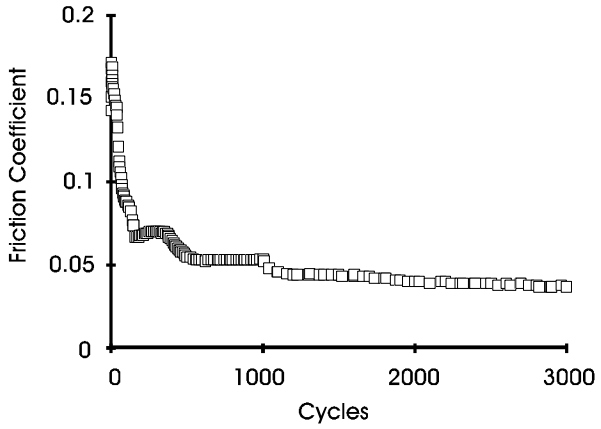

Figure 1. Typical reciprocating ball-on-flat friction vs. endurance results for steel sliding against IBD Pb-Mo-S in a dry air environment.

3.2. Analyses

3.2.1 As-deposited coating

The coatings were specular and almost always near full theoretical density. RBS depth profiling revealed that the target configuration of MoS_2 and Pb produced coatings having relatively uniform Pb:S:Mo ratios throughout the coating, with S:Mo ratios from 1.6 to 1.8. On the other hand, when the Pb and composite Mo-S targets were used, sulfur concentration was high at the substrate-coating interface (interface S:Mo ratios ranged from 5 to 10), but decreased throughout the coating to the surface; average S:Mo ratios were from 2.8 to 6.0. The variation in S content in the coatings made with the composite Mo-S target is attributed to depletion of the S contained in holes in the target [14]. In both target configurations, the Pb concentration was found to be approximately uniform throughout the coating thickness. Carbon content is also typically low (~2%). However, Auger depth profiling indicated that coatings made with the MoS_2 target had as much as 10% C content. This resulted from unintentional sputtering of graphite from the shield surrounding the molybdenite target due to beam broadening when the sputtering power was increased.

As-deposited IBD Pb-Mo-S coatings were examined by XRD and found to be amorphous. XRD spectra from an IBD Pb-Mo-S coated substrate and two substrates with IBAD MoS_2 coatings, (A and B), are shown in Figure 2. Basal (002) peaks are observed in IBAD MoS_2 coating A, indicating a crystalline MoS_2 coating [22]; in contrast, IBAD MoS_2 coating B and the IBD Pb-Mo-S coating exhibit only substrate peaks, consistent with an amorphous coating structure.

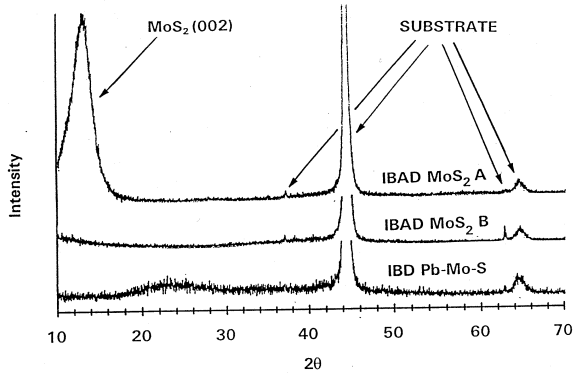

Figure 2. XRD spectra of IBAD MoS_2 (A and B) and IBD Pb-Mo-S coatings on M50 steel.

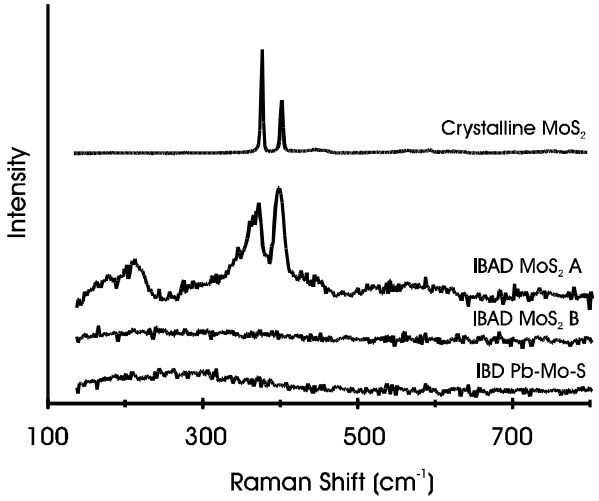

Micro-Raman spectra from the same three coatings and molybdenite powder are shown in Figure 3. The spectrum from the crystalline IBAD MoS_2 (A) coating exhibits bands similar to those found in molybdenite [23]. In contrast, the micro-Raman spectra obtained from the amorphous IBAD MoS_2 (B) and IBD Pb-Mo-S coatings are featureless.

3.2.2 Wear tracks on coatings and ball transfer films

3.2.2.1 Micro-Raman and optical microscopy

Micro-Raman spectroscopy of tracks on IBD Pb-Mo-S coatings showed bands similar to those observed for crystalline IBAD MoS_2; typical examples are shown in Figure 4 along with a spectrum from the as-deposited coating for reference. Micro-Raman scans of wear track surfaces showed MoS_2 Raman bands in smooth regions of the tracks. These MoS_2 bands were observed in wear tracks after as few as 100 sliding cycles, as well as on worn material at the ends and sides of the wear tracks. No other wear products which could have formed during

sliding in air, such as the oxidation products of Pb and Mo (MoO_2, MoO_3, $PbMoO_4$, PbO, etc.), were detected in any of the wear tracks or wear debris. We note, however, that increasing the laser intensity resulted in oxidation (e.g. to $PbMoO_4$) which was easily observed in the Raman spectra. PbS, another potential material present, has no first order Raman modes and is therefore not observable via Raman spectroscopy [10].

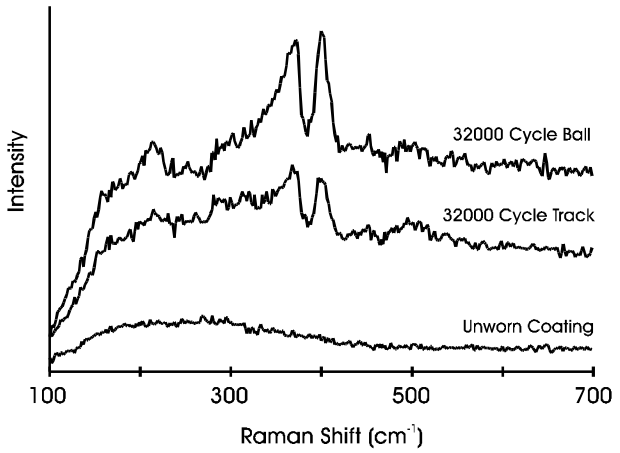

Figure 4. Micro-Raman spectra obtained from unworn IBD Pb-Mo-S coating as well as wear track and ball surfaces (after 32000 recriprocating sliding cycles).

Optical microscopy of transfer films on balls indicated three distinct regions near the contact zone, similar to those described previously for MoS_2 [24]; a photomicrograph of a steel ball after 3000 reciprocating sliding cycles against a 20 at.% Pb IBD Pb-Mo-S coating is shown in Figure 5. The center region consists of a circular region with a non-uniform transfer layer. The second area, the leading/trailing edges (which alternate in reciprocating sliding tests), contains compacted wear particles that appear smooth and gray. Surrounding the contact area is a region containing loose, powdery debris.

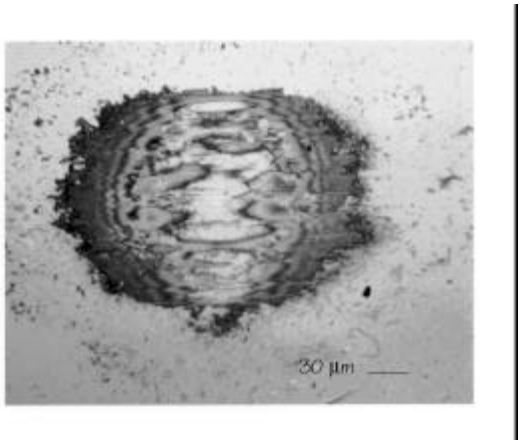

Figure 5. Optical micrograph of contact area on 52100 steel ball after 3000 reciprocating sliding cycles against IBD Pb-Mo-S coated steel.

Micro-Raman spectroscopy showed MoS_2 Raman bands on balls at both early (300 cycles) and late (32000 cycles) stages of sliding. MoS_2 Raman bands were observed both in the center of the transfer film (contact zone) as well as in thicker areas of compacted debris at the leading/trailing edges outside the contact zone. Debris particles found on the balls gave featureless Raman spectra. As on the tracks, no other wear products which could have formed during sliding in air (MoO_2, MoO_3, $PbMoO_4$, PbO, etc.) were observed on any of the balls.

3.2.2.2 Auger microscopy

Scanning Auger microscopy was used to investigate the surface composition of wear tracks and ball transfer films after various stages of sliding. Auger analysis of the track and ball surfaces (without sputtering) showed the coating elements Pb, S and Mo, as well as C and O. Here we report only on S:Mo ratio in order to elucidate the Raman findings of crystalline MoS_2; details of the other constituents (Pb, O, C) are left to a future paper. A comparison of Auger S:Mo concentration ratios for IBD Pb-Mo-S and IBAD MoS_2 coatings are shown in Table 4. The IBD Pb-Mo-S coating tested had a higher S concentration than the IBAD MoS_2 coating, therefore the higher S:Mo ratios at the track surface is not unexpected. Transfer films on ball surfaces showed similar S:Mo ratios to the track surface, consistent with *in situ* analysis of sputtered MoS_2 coatings run in vacuum [25]. IBD Pb-Mo-S transfer films had a wider variation in S:Mo ratios. This can be accounted for by variation in O and Pb contents of the transfer material. Importantly, the data shows that both S and Mo are present in the outermost 1-2 nm of the track and ball surfaces.

Table 4.
S:Mo ratios of ball and track surfaces by Auger analysis

Coating	Cycles	S:Mo Ratio	
		Track	Ball
IBD Pb-Mo-S	1000	2.3	–
	2300	3.2	2.5 – 4.5
	32000	3.2	1.1 – 2.5
IBAD MoS_2	1000	2.6	–
	3000	2.6	2.6 – 2.8

4. Discussion

An important result of this study is that IBD Pb-Mo-S coatings have improved endurances over unalloyed IBAD MoS_2 coatings. In dry sliding tests, IBD Pb-Mo-S solid lubricating coatings with Pb contents from 4-26 at.% resulted in endurances which were on average more than 2 times greater than that of IBAD MoS_2. In fact, the IBD Pb-Mo-S coatings, which were deposited without the aid of an assist ion source, performed even better than the

optimized IBAD MoS_2 coatings. Additionally, in earlier rolling tests IBAD MoS_2 coatings were shown to provide better endurances than both burnished and rf-sputtered MoS_2 films [26]. Recently, rolling tests showed that the best performing IBD Pb-Mo-S coating (466 krev in sliding contact, Table 1) outperformed all previously tested coatings (burnished, sputter deposited, multilayered with Au/Pd, Ni), having an endurance of 10 million revolutions [27].

As can be seen from Tables 1 and 2, there is a relatively large scatter in endurance of coatings deposited under similar conditions. These differences may be due to variability in tribotesting, coating adhesion or other coating properties; the latter two may be related to observed variations in coating composition, which could either enhance or detract from coating performance. For example, significant gradation of S content was observed in the coatings made using the composite Mo-S target. Also, coatings made with the MoS_2 target had high (10% or more) C content but no structural differences to other IBD Pb-Mo-S coatings. This carbon content is not necessarily detrimental; it has been previously noted that additions of graphite to MoS_2 can improve lubricant performance [1,28]. Despite the scatter, the 17 IBD Pb-Mo-S coatings studied provide clear improvements over even the 29 optimized IBAD MoS_2 coatings in endurance testing.

Ball-on-disk friction coefficients for IBD Pb-Mo-S coatings were also low (except for the 50 at.% Pb coating), falling within the range of friction coefficients observed for IBAD MoS_2 coatings, ~0.02 or lower. Interestingly, the observed values for interfacial shear strength S_o (8 - 15 MPa) for the IBD Pb-Mo-S coatings are at the low end of values obtained for the IBAD and sputtered MoS_2 coatings. In fact, these values are almost as low as observed for sputtered MoS_2 tested in high vacuum (7 MPa) [17,29]. Clearly, the presence of even substantial amounts (as high as 26 at.%) of Pb in the bulk coating does not prevent the development of easily sheared interfaces and low friction sliding.

The similarities in tribological behavior of the IBD Pb-Mo-S and IBAD MoS_2 coatings can be associated with sliding-induced changes occurring at the ball/coating interface. While the unworn IBD Pb-Mo-S coatings are amorphous via XRD and exhibit featureless Raman spectra, both wear tracks and transfer films on balls provide Raman spectra consistent with that of crystalline MoS_2. This implies that sliding induces ordering in IBD Pb-Mo-S, resulting in material containing crystalline MoS_2. Similar sliding-induced crystallinity has been observed by Zabinski et al. [10] in PbO:MoS_2 coatings via Raman spectroscopy. The present results, in fact, suggest that this crystallization can take place after a small number of sliding cycles (as low as 100).

It is important to note that low friction was obtained despite the fact that the coating is initially amorphous. It was once believed that amorphization destroyed the lubricity of MoS_2[5]. However, more recent evidence from studies of ion-beam modified MoS_2 contradicts this hypothesis [13,30]. In the present experiment, MoS_2 is observed via micro-Raman spectroscopy in ball transfer material and on the wear tracks of IBD Pb-Mo-S coatings. In fact, the MoS_2 is observed on track surfaces after as few as 100 reciprocating sliding cycles, at which time the friction coefficient is near the steady state value. Based on experimental (<55 nm) and calculated (~35 nm) depth sensitivities for Raman spectroscopy of MoS_2, crystalline (transformed) MoS_2 can be found within ~40 nm of the surface. In addition, Auger analyses of the worn surfaces demonstrated the presence of S and Mo at sufficient stoichiometry to provide MoS_2 in the near surface region (top 1–2 nm) of both ball and track surfaces. Therefore, experimental evidence suggests that the lubricity of the initially amorphous coating is related to the tribomechanical formation of crystalline MoS_2 at the sliding interface.

What causes the recrystallization? Sliding at the slow sliding speeds (4 mm/sec) used here and with friction coefficients below 0.03 is expected to cause a temperature rise less than a few degrees. Furthermore, the coatings were exposed to temperature rises of as much as 60°C during deposition as a result of ion-beam heating, yet no crystallinity was observed in the as-deposited coatings. Hence, thermally-induced crystallization is not likely. Hilton and Fleischauer [31] have observed sliding-induced crystallization (via XRD) of MoS_2 coatings having no initial long-range order, suggestive of stress-induced recrystallization. We speculate as well that crystallization of IBD Pb-Mo-S coatings may be due to mechanical stresses. In addition, it is well known that MoS_2 crystallites, from powders [32] to sputtered coatings [24,33], reorient during sliding to have basal planes parallel to the sliding direction. The issues of whether these stresses crystallize MoS_2 directly, or indirectly (e.g. by causing local phase separation of Pb from the MoS_2), whether there is preferential orientation of the crystallized material, and to what depth the MoS_2 transformation occurs, are left for future investigations.

The presence of crystalline MoS_2 can account for low friction coefficients; however, the role of Pb in the friction behavior is less clear. Certainly, the presence of other components (e.g. Pb,O) in the region may increase friction when present in some critical quantity. In our case, a 50 at.% Pb coating had a higher friction coefficient and low wear life; hence, IBD Pb-Mo-S coatings in this study can accommodate at least 26 at.% Pb and still provide low friction coefficients. Other researchers have also observed low friction in MoS_2 alloyed with different materials including PbO, where coatings with PbO:MoS_2 ratios as

high as 1:1 can provide low friction [10]. Similarly, Peterson [34] has shown in sliding experiments that MoS_2 powders can accommodate large amounts of MoO_3 powders (over 90%) before substantial increases in friction are observed. Additionally, low friction sliding can be maintained against MoS_2 coatings even though the interfacial transfer films contain MoO_3 as well as oxides of the slider material [24,35]. Alternatively, formation of other lubricious compounds like $PbMoO_4$ is possible. Zabinski et al. [10] have observed $PbMoO_4$ in wear debris formed after sliding against PbO-MoS_2 composite coatings under similar contact stresses to the present investigation; the presence of substantial amounts of O in their coatings may enhance the formation of such oxide compounds. The present results, however, show low friction behavior without the formation of this crystalline oxide phase. Moreover, $PbMoO_4$ alone is not an effective lubricant at room temperature [36,37]. It is possible that Pb plays little or no role in the low friction, so that what dominates the friction behavior is the ability of MoS_2 to incorporate other materials as benign components while maintaining low friction.

We speculate that the good friction properties and high endurance of these initially amorphous IBD Pb-Mo-S coatings can be related to the following attributes: First, the IBD coatings are initially dense and adherent; these properties have been shown to improve wear life [30,38]. Second, sliding on the IBD Pb-Mo-S material produces surfaces containing crystalline MoS_2. Additionally, the sliding interface has low shear strength S_o. The combination of dense, adherent coatings with formation of easily-sheared, MoS_2-containing sliding surfaces results in the wear resistance and low friction properties of IBD Pb-Mo-S coatings under sliding contact conditions.

While the low friction and good endurance can be accounted for by the preceding arguments, the *improved* performance of a number of the Pb-containing coatings over IBAD MoS_2 can not. The nature of the contribution of Pb to the improved endurance of IBD coatings is not yet clear. Early work incorporating metal additives to rf-sputtered MoS_2 coatings showed improved friction and endurance, which was attributed to increased crystallite size and hardness [4] and coating densification and cohesivity [5]. More recently, improvements in performance of sputtered coatings have been obtained by laser annealing of Au:MoS_2 [8,9] and deposition of metal multilayered structures (which suppresses edge crystallite growth) [7], both of which result in coating densification. While densification, increased crystallite size, and improved crystallite orientation can all contribute to increased performance of sputtered coatings, the IBD Pb-Mo-S coatings deposited in this study are amorphous, have theoretical coating densities not unlike their IBAD MoS_2 counterparts, yet out perform them. It is possible that Pb changes the mechanical properties (e.g. hardness, elastic modulus, and fracture toughness) or the tribomechanical wear processes (e.g. oxidation or wear debris formation [39]). Either of these conditions could lead to increased coating wear performance; these issues of mechanics and tribochemistry will be addressed in future work.

5. Conclusions

1. The addition of Pb to IBD MoS_2 coatings enhanced high stress, dry sliding coating wear life by more than a factor of 2 over optimized IBAD MoS_2 coatings.

2. Steady-state friction coefficients and shear strengths of the IBD Pb-Mo-S coatings against steel were as low as observed in unalloyed MoS_2 coatings.

3. Sliding produced crystalline MoS_2 on the initially amorphous IBD Pb-Mo-S coating surface. Sliding also produces a transfer film containing crystalline MoS_2 on the ball surface.

4. The wear resistance and low friction properties of IBD Pb-Mo-S coatings are attributed to the combination of dense, adherent coatings and formation of easily-sheared, MoS_2-containing sliding surfaces.

Acknowledgments

The authors would like to acknowledge the assistance of J.C. Wegand and A.M. Solow for some of the tribotesting, as well as C.R. Gossett for RBS analyses. The authors would also like to acknowledge ONR for funding the micro-Raman study and I.P. Hayward for assistance with the micro-Raman spectroscopy. K.J.W. would like to thank the National Research Council for support through a post-doctoral fellowship.

References

[1] M.J. Devine, E.R. Lamson, and J.H. Bowen, Jr., *J. Chem. Eng. Data* **6** (1961) 79-82.
[2] W.J. Bartz, R. Holinski, and J. Xu, *Lubr. Eng.* **42** (1986) 762-769.
[3] P.W. Centers and F.D. Price, *Wear* **129** (1989) 205-213.
[4] B.C. Stupp, *Thin Solid Films* **84** (1981) 257-266.
[5] T. Spalvins, *Thin Solid Films* **118** (1984) 375-384.
[6] P. Niederhäuser, H.E. Hintermann, and M. Maillat, *Thin Solid Films* **108** (1983) 209-218.
[7] M.R. Hilton, R. Bauer, S.V. Didziulis, M.T. Dugger, J.M. Keem, and J. Scholhamer, *Surf. Coat. Technol.* **53** (1992) 13-23.
[8] L.E. Pope, T.R. Jervis, and M. Nastasi, *Surf. Coat. Technol.* **42** (1990) 217-225.
[9] T.R. Jervis, J.-P. Hirvonen, and M. Nastasi, *J. Mater. Res.* **6** (1991) 1350-1357.
[10] J.S. Zabinski, M.S. Donley, V.J. Dyhouse, and N.T. McDevitt, *Thin Solid Films* **214** (1992) 156-163.

[11] N.T. McDevitt, M.S. Donley, and J.S. Zabinski, *Wear* **166** (1993) 65-72.
[12] R.N. Bolster, I.L. Singer, J.C. Wegand, S. Fayeulle, and C.R. Gossett, *Surf. Coat. Technol.* **46** (1991) 207-216.
[13] L.E. Seitzman, R.N. Bolster, I.L. Singer, and J.C. Wegand, *Tribo. Trans.*, in press.
[14] R.N. Bolster, NRL Report MR/6176-92-7135 (1992).
[15] L.E. Seitzman, I.L. Singer, R.N. Bolster, and C.R. Gossett, *Surf. Coat. Technol.* **51** (1992) 232-236.
[16] R.C. Bowers and W.A. Zisman, *J. Appl. Phys.* **39** (1968) 5385.
[17] I.L. Singer, R.N. Bolster, J.C. Wegand, S. Fayeulle, and B.C. Stupp, *Appl. Phys. Lett.* **57** (1990) 995-997.
[18] I.L. Singer, in *Fundamentals of Friction: Macroscopic and Microscopic Processes*, I.L. Singer and H.M. Pollock (eds.), Kluwer, Dordrecht, Netherlands, 1992, 237-261.
[19] M.P. Seah, in *Practical Surface Analysis, Vol. 1: Auger and X-ray Photoelectron Spectroscopy*, D. Briggs and M.P. Seah (eds.), Wiley, New York, NY, 1990, pp. 201-255.
[20] M.V. Klein, *Optics*, Wiley, New York, NY, 1970, p.534.
[21] B.L. Evans and P.A. Young, *Proc. Roy. Soc. A* **284**, (1965) 402-422.
[22] L.E. Seitzman, R.N. Bolster, and I.L. Singer, *Surf. Coat. Technol.*, **52** (1992) 93-98.
[23] T.J. Weiting and J.L. Verble, *Phys. Rev. B.* **3** (1971) 4286-4292.
[24] S. Fayeulle, P.D. Ehni, and I.L. Singer, in *Mechanics of Coatings*, Leeds-Lyon 16, Tribology Series 17, Dowson, D, Taylor, C.M. and Godet, M. (eds.), Elsevier Science Publishers B.V., 1990, 129-138.
[25] P.D. Ehni and I.L. Singer, in *New Materials Approaches to Tribology: Theory and Applications, MRS Symp.*, Vol. 140, L. Pope, L. Fehrenbacher, and W. Winer (eds.), Materials Research Society, Pittsburgh, PA, 1989, pp. 245-249.
[26] S.V. Didziulis, M.R. Hilton, R. Bauer, and P.D. Fleischauer, Aerospace Report No. TOR-92(2064)-1, 1992.
[27] I.L. Singer, R.N. Bolster, L.E. Seitzman, K.J. Wahl, M.B. Peterson, and R.L. Mowery, NRL Report (# to be added to galley proof).
[28] M.N. Gardos, *Tribo. Trans.* **31** (1987) 214-227.
[29] E.W. Roberts, *Proceedings of the Institute of Mechanical Engineering Tribology-Friction, Lubrication and Wear, Fifty Years On*, Institute Mechanical Engineering, London, 1987, 503.
[30] N.J. Mikkelsen, J. Chevallier, G. Sørensen, and C.A. Straede, *Appl. Phys. Lett.* **52** (1988) 1130-1132.
[31] M.R. Hilton, and P.D. Fleischauer, in *New Material Approaches to Tribology: Theory and Applications, MRS Symp.*, Vol. 140, L. Pope, L. Fehrenbacher, and W. Winer (eds.), Materials Research Society, 1989, 227-238.
[32] R.F. Deacon, and J.F. Goodman, *Proc. Roy. Soc. A* **243** (1958) 464-482.
[33] P.D. Fleischauer and R. Bauer, *ASLE Trans.* **31** (1988) 239-250.
[34] M.B. Peterson, personal communication, Wear Sciences Corp., Arnold MD 21012.
[35] S. Fayeulle, P.D. Ehni, and I.L. Singer, *Surf. Coat. Technol.* **41** (1990) 93-101.
[36] M.B. Peterson, S.F. Murray, and J.J. Florek, *ASLE Trans.* **2** (1960) 225-234.
[37] M.B. Peterson, S.B. Calabrese, and B. Stupp, ARPA Report, Contract No. N00014-82-C-0247, 1982.
[38] J. Chevallier, S. Olesen, G. Sørensen, and B. Gupta, *Appl. Phys. Lett.* **48** (1986) 876-877.
[39] I.L. Singer, *Surf. Coat. Technol.* **49** (1991) 474-481.